ELSEVIER

Journal of Nuclear Materials 299 (2001) 242–249

journal of nuclear materials

www.elsevier.com/locate/jnucmat

Tritium recovery from nanostructured $LiAlO_2$

L.M. Carrera [a,*], J. Jiménez-Becerril [a], R. Basurto [a], J. Arenas [b], B.E. López M [a], S. Bulbulian [a], P. Bosch [c]

[a] *Departamento de Química, Instituto Nacional de Investigaciones Nucleares, A.P. 18-1027, C.P. 11801, México, D.F., Mexico*

[b] *Departamento de Síntesis y Caracterización de Materiales, Instituto Nacional de Investigaciones Nucleares, A.P. 18-1027, C.P. 11801, México, D.F., Mexico*

[c] *Universidad Autónoma Metropolitana, Iztapalapa, Departamento de Química, A.P. 55-532, C.P. 09340, México, D.F., Mexico*

Received 26 March 2001; accepted 23 August 2001

Abstract

In this work, a complex superlattice is obtained from a simple synthesis method. A detailed study by X-ray diffraction and electron microscopy is presented to determine the structural composition and the nanostructure of the obtained $LiAlO_2$ mixtures. To establish the influence of the superlattice presence in the tritium recovery, the obtained samples were irradiated with a mixed thermal and fast neutron flux in the nuclear reactor Triga Mark III (NRTMIII) at Salazar, Mexico. The study is focused on the superlattice effect on tritium mobility.

1. Introduction

Lithium ceramics are refractory materials and provide tritium after neutron irradiation [1]; they can, then, be used as tritium breeding material in a fusion device [2] to supply tritium to the plasma fuel and heat for the power generator systems. Tritium is produced by the nuclear reaction: $^6Li(^1n,\alpha)^3H$. As 7.5 wt% of natural lithium ($^6Li + {}^7Li$) is ^6Li, then all lithium ceramic materials as Li_2O, $LiAlO_2$, Li_2ZrO_3 or Li_4SiO_4 will produce tritium [3]. The use of one of them depends on the release behavior of the produced tritium in each solid breeder material. The release behavior of all considered lithium ceramic breeder materials has not been fully understood. Results of in situ release experiments have been mainly analyzed assuming that the overall release process of tritium was mainly controlled by the tritium diffusion in the crystal grain [4]. Nevertheless, other processes like surface reaction on the grain, diffusion through pores of sintered particles and diffusion through the boundary layer formed on the particle surface must be considered. Still, some reactions between purge gas and the compounds present on the surface may also alter the tritium production [5].

$LiAlO_2$ possesses thermophysical, chemical and mechanical stability at high temperature [6,7]. This aluminate may crystallize as α, β or γ phase. This later phase is the main crystallographic form found at high temperatures, indeed, it possess a somewhat higher melting point of 1880 K. The γ-$LiAlO_2$ may be described by the space group $P4_12_12$, or its enantiomorph $P4_32_12$ [8] in which lithium and aluminum atoms are in the special positions (4a) and oxygen atoms in the general positions (8b). The cell parameters are $a = 51.687 \pm 0.005$ nm and $c = 62.679 \pm 0.006$ nm. Lithium and aluminum ions are both in tetrahedral coordination with oxygen ions.

Marezio and Remika [9] have found that α-$LiAlO_2$ has a space group $R\bar{3}m$. The symmetry atoms are found along the z-axis. Cell parameters are $a = 28.003 \pm 0.006$ nm and $c = 142.16 \pm 0.03$ nm. In α-$LiAlO_2$ lithium and aluminum are octahedrally co-ordinated. It is possible to obtain γ-$LiAlO_2$ from pure α-$LiAlO_2$, which is cold pressed and sintered at 1373 K. The α to γ phase transformation is irreversible, though some α-$LiAlO_2$ has been made from γ-$LiAlO_2$ by subjecting samples to high pressures and temperatures [10]. α- and γ-$LiAlO_2$

* Corresponding author.
E-mail address: lcg@nuclear.inin.mx (L.M. Carrera).

0022-3115/01/$ - see front matter
PII: S0022-3115(01)00693-6

can co-exist and its performance as tritium breeder material has been investigated [11].

Not only the α, β and γ-$LiAlO_2$ may be found, more complex structures have been reported. Superlattices [12] in γ-$LiAlO_2$ has been produced by electron irradiation, no correlation has been established between the tritium recovery and these nanostructural features.

In a previous paper we found that the crystallite size and morphology, as well as the fraction of γ-$LiAlO_2$, depended on the synthesis method [13]. However, the microstructure of the obtained $LiAlO_2$ mixtures was not determined. It seems, then, that correlation between the synthesis method of $LiAlO_2$ and the structural features (crystalline as well as nanostructural) may contribute to a better understanding of tritium release. In this work, we discuss how superlattice nanostructure may modify tritium release.

2. Experimental

2.1. $LiAlO_2$ preparation

Lithium aluminate samples were synthesized following two conventional procedures: solid-state reaction (Sos synthesis), or precipitation from peroxide (Per synthesis).

2.1.1. Sos synthesis

The Sos sample (solid state) was obtained when equimolar amounts of γ-Al_2O_3 and Li_2CO_3 were mixed in acetone for 30 min. Acetone was evaporated and the resulting solid was dried at 373 K for 3 h. The white powder was, then, calcined at 1073 K for 4 h and, then, at 1273 K for 1 h.

2.1.2. Per synthesis

The Per sample (peroxide) was obtained when equimolar amounts of γ-Al_2O_3 and Li_2CO_3 were mixed in 20 ml of distilled water added to 20 ml of a 30% H_2O_2 solution. The Li_2CO_3 was decomposed in the solution and Li_2O_2 was obtained. The resulting mixture was heated at 308 K for 5 min until the reaction began, the heating was, then, stopped and the solution was stirred until the reaction was finished. The excess water was evaporated and the solid was dried at 373 K for 3 h. The resulting white powder was calcined at 1073 K for 4 h and, then, at 1273 K for 1 h.

2.2. Tritium production

Tritium was produced by neutron irradiation of 100 mg of the prepared lithium aluminate ceramics. The Sos and Per samples, sealed in plastic bags, were irradiated simultaneously (2 h) in a fixed irradiation system of the nuclear reactor with a mixture of thermal (1.4765×10^{20} nm^{-2}, $0 \leqslant E \leqslant 0.4$ eV) and fast (5.8813×10^{19} nm^{-2}, 0.4 eV $< E \leqslant 10$ MeV) neutron fluence. The nuclear reactor is a Triga Mark III at Salazar, Mexico, inside the core of the reactor the coolant temperature is about 343 K. The neutron fluences were determined using the Al (99%)–Au (1%) thin foils activation method. The thin foils, wrapped up in absorbent paper and held in a container with adhesive tape, were placed in the following order: a bare thin foil next to a thin foil with both sides cadmium covered; these cadmium covered foils were also wrapped up in absorbent paper. The later foils react with neutrons with energies greater than 0.48 eV i.e., fast neutrons. To cover all the interest area in the fixed irradiation system a total of 10 thin foils were used, half of them cadmium-covered. This arrangement was irradiated during 30 min in the fixed irradiation system in a reactor power level of 1000 kW. After being exposed to neutrons in the fixed irradiation system the thin foils were analyzed by γ-spectrometry using an hyperpure germanium detector coupled to a pulse height analyzer [14]. The obtained results were used to obtain the thermal and fast neutron fluxes [15].

2.3. Tritium recovery

The neutron irradiated lithium aluminate samples (100 mg each) were introduced into stainless steel tubes and were heated at 773 K for 20–345 min. Tritium was swept with Ar plus 0.1 H_2 as gas carrier. The outlet gases from the heating stainless steel tube were passed through a heated CuO bed to ensure that all of the tritium is oxidized, then the tritium species, HTO were collected into aqueous cold traps (278 K).

Tritium activity released in each sample was expressed as a fraction of the total activity. The recovery of tritium from the solid was determined by measurements in both the aqueous solution and the solid. Tsuchiya et al. [16] dissolved the $LiAlO_2$ powder with HNO_3, in the present paper solid lithium aluminate was complete dissolved in a 50% H_2SO_4 solution. Tritium was determined by liquid scintillation spectrometry in a Packard Tri-Carb 2700TR equipment.

2.4. Characterization

A Siemens D500 diffractometer coupled to a copper anode X-ray tube was used to obtain the experimental X-ray diffraction patterns. The wavelength $K_{\bar{\alpha}}$ was selected with a diffracted beam monochromator. The X-ray tube was operated at 35 kV and 20 mA. All diffraction patterns were obtained in scanning mode with a 0.02° (2θ) step size. Crystalline compounds were identi-

fied conventionally with the JCPDS files. The diffraction patterns of the original samples Sos and Per were refined using the Rietveld method. All refinements were obtained using the DBWS-9006PC [17] and WYRIET [18] computer programs. The α-$LiAlO_2$ and the γ-$LiAlO_2$ structures as well as the atom positions were initially assumed to be those proposed by Marezio [8,9] for both structures.

All electron diffraction patterns were obtained by using a Jeol 100CX transmission electron microscope (TEM). The samples were supported on copper grids (300 mesh) and covered with a carbon film. To determine superlattice structure an electron diffraction simulation were made using the Cerius computer package [19]. It was assumed that the Per sample crystallizes as a layered ultrathin coherent structure (LUCS) [20]; then, the problem was only to find the crystallographic planes in which the α-$LiAlO_2$ and the γ-$LiAlO_2$ can form such type of structure.

A Jeol JSM-5200 scanning electron microscope (SEM) was used to determine the sample morphology. To obtain materials electrically conductive, all samples were covered with a thin silver film using a Jeol (JFC-1100) fine coat ion sputter.

3. Results

Both syntheses provided a solid-state mixture of various crystalline compounds as shown by the original X-ray diffraction patterns in Figs. 1 and 2. The diffractogram peaks were always sharp and well defined. No contribution from any non-crystalline compound was observed. Detailed information for the Sos and the Per samples is given in Table 1. To determine the structural parameters and the γ- and α-$LiAlO_2$ phase content

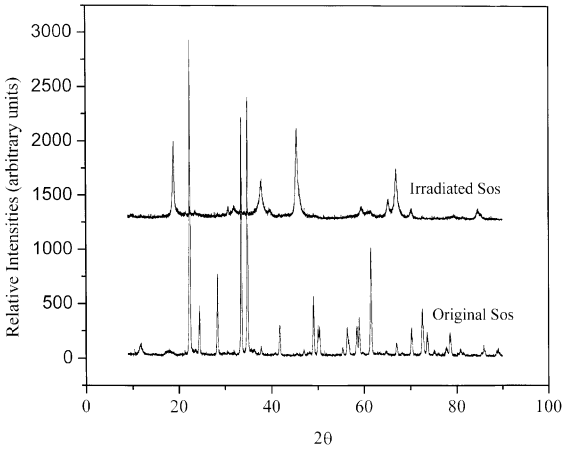

Fig. 1. Powder diffraction patterns of the original and irradiated Sos samples.

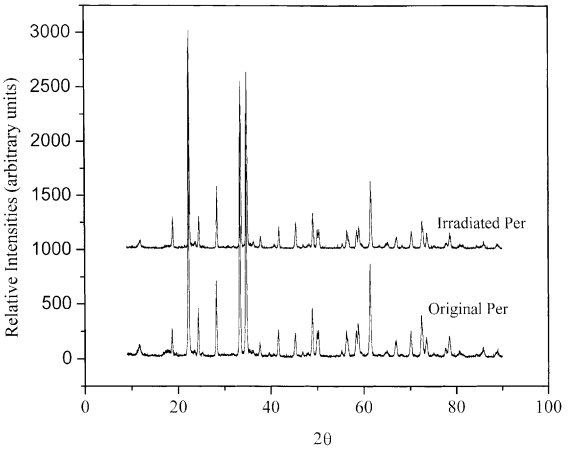

Fig. 2. Powder diffraction patterns of the original and irradiated Per samples.

Table 1
Composition (wt% ±1) of Sos and Per original samples

Crystalline compound	Sos (wt%)	Per (wt%)
γ-$LiAlO_2$	94.5	91.3
α-$LiAlO_2$	0	5.7
Li_2O_2	0	<3
$LiH(AlO_2)_2 \cdot 5H_2O$	≅5.5	<3

(wt%) of the obtained compounds, Rietveld refinement was used.

For the Sos sample, if only the presence of γ-$LiAlO_2$ is assumed, a simulated powder diffraction pattern with a satisfactory Rietveld fitting parameter $R - WP = 18.5$ is obtained. The refined cell parameters were $a = 51.6 \pm 0.3$ nm and $c = 62.7 \pm 0.2$ nm. This result indicates a fairly small relaxation in the unit cell (Marezio [8] values were $a = 51.6$ nm and $c = 62.6$ nm), the density was 2.62 g/cm^3, and the Rietveld calculated γ-content was 94.5 wt%.

Although it is more common for preparations such as this to form $LiAl_2(OH)_7 \cdot 5H_2O$ [21], only $LiH(AlO_2)_2 \cdot 5H_2O$ was identified. Frianeza-Kullberg et al. [22] also found this latter compound.

Table 1 shows that Per sample is a complex oxide as it is constituted at least by four compounds (γ-$LiAlO_2$, α-$LiAlO_2$, Li_2O_2 and $LiH(AlO_2)_2 \cdot 5H_2O$). If only γ-$LiAlO_2$ and α-$LiAlO_2$ were considered in the Rietveld fitting, $R - WP$ turned out to be 16.08. Again, the γ phase has cell parameters $a = 51.6$ nm and $c = 62.7$ nm (tetragonal symmetry). The resulting density was 2.62 g/cm^3 which, as expected, is the same value found in the Sos sample.

The obtained α-$LiAlO_2$ whose cell parameters were $a = 28.0$ nm and $c = 142.1$ nm corresponds to the symmetry proposed by Marezio et al. [9]. ($R - 3$ M,

hexagonal symmetry, and $a = 28.003 \pm 0.006$ nm and $c = 142.16 \pm 0.03$ nm.) The density was, in this case, 3.40 g/cm^3 which is in agreement with the values reported by Marezio et al. [9]. The Rietveld calculated γ and α contain were 91.3 and 5.7 wt%, respectively.

To determine if transitions order–disorder, often found in ceramics, were present a microscopically study was performed. This technique was focused on the study of γ- and α-$LiAlO_2$ compounds present in the samples.

In Sos sample three types of electron diffraction patterns were found, well defined nanostructures corresponding to polycrystallites, monocrystallites and large ordered domains of γ-$LiAlO_2$. The spot diffraction pattern in Fig. 3 corresponds to a monocrystalline zone of γ-$LiAlO_2$ phase, the intensity of the spots suggests the presence of defects. Therefore γ-$LiAlO_2$ crystallites do not seem to be structurally homogeneous.

For Per sample there were only two well defined nanostructures: single crystal of γ-$LiAlO_2$ zones and $\gamma + \alpha$-$LiAlO_2$ superlattice zones, Fig. 4. The intense spots from the fundamental γ-$LiAlO_2$ lattice are surrounded by fainter spots of α-$LiAlO_2$ lattice. Both pictures were taken from the same sample area, again γ-phase crystallites seemed to be heterogeneous but in this case α-phase was intimately linked to the γ-phase, showing the presence of a superlattice. To define the type of superlattice an ultrathin layered structure was proposed. This structure is constituted by three layers of α-$LiAlO_2$ followed by 20 layers of γ-$LiAlO_2$ with interface between $(1\,1\,0)_\gamma$ and $(0\,0\,1)_\alpha$ crystalline planes. Fig. 5 shows the corresponding simulated electron diffraction pattern obtained with zone axis (1 1 3).

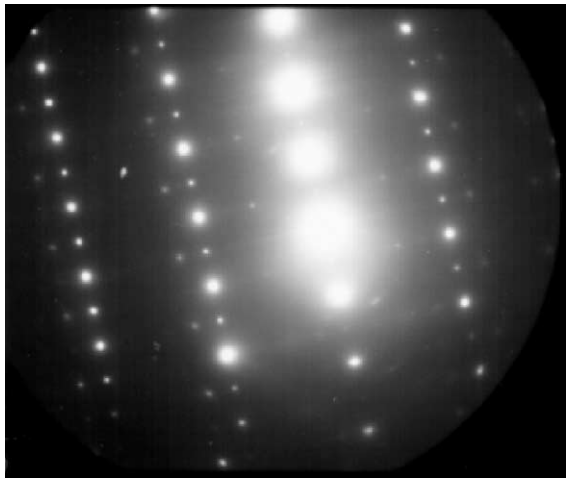

Fig. 4. Superlattice in Per sample. The intense spots from the fundamental γ-$LiAlO_2$ lattice are surrounded by fainter spots of α-$LiAlO_2$ lattice.

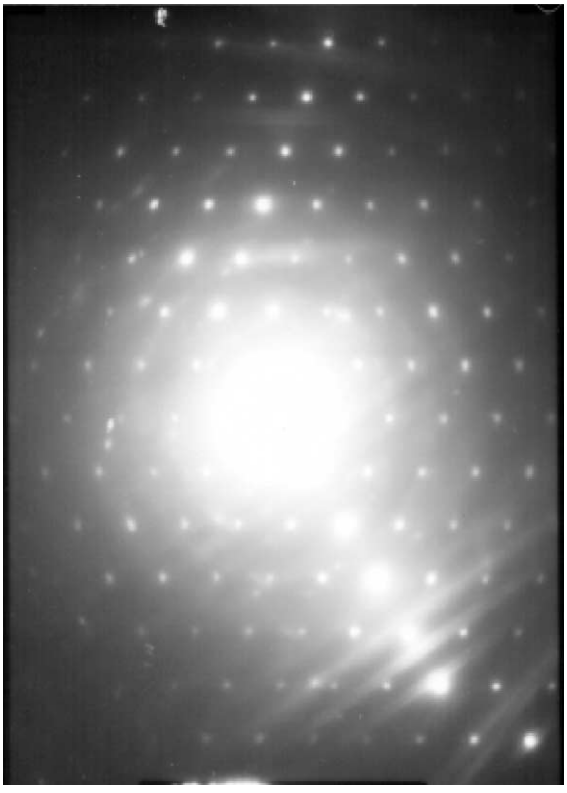

Fig. 3. Spot diffraction pattern corresponding to a monocrystalline zone of γ-$LiAlO_2$ phase Sos sample.

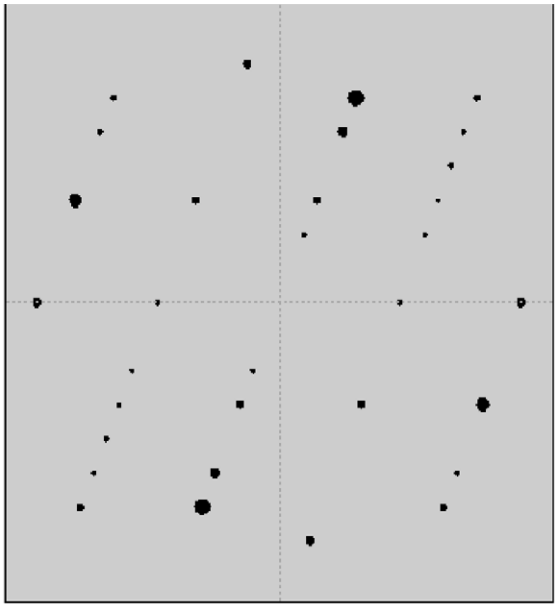

Fig. 5. Simulated electron diffraction pattern of superlattice in Per sample.

The morphology of a typical agglomerate of the ceramics produced by the Sos synthesis is shown in Fig. 6. These agglomerates (mean diameter ≈0.19 nm) were constituted by hexagonal particles whose diameter and height were around 0.12 and 0.02 nm.

In the Per synthesis, Fig. 7, only some crystals presented a hexagonal shape. The agglomerates (mean diameter ≈ 0.206 nm) were mainly constituted by smaller particles, whose size was close to 0.01–0.02 nm and whose shape was not well defined. Hence, although α and γ phases were present (X-ray diffraction results) they cannot be morphologically distinguished. The grain size of this sample was larger than the Sos sample: if compressed, the Sos sample produced better pellets.

Figs. 1 and 2 compare the X-ray diffraction patterns of the original and the irradiated samples, Sos and Per, respectively. After irradiation with a lithium burn up of 1.3×10^{-3}% the γ-$LiAlO_2$ phase is transformed to α-$LiAlO_2$ phase, Fig. 1. In the case of the Per samples, no change of phase occurred but the α-$LiAlO_2$ phase content increased, Fig. 2. Detailed composition for the Sos and the Per irradiated samples is given in Table 2. These transformations are found to be stable. No reversible transformations were observed.

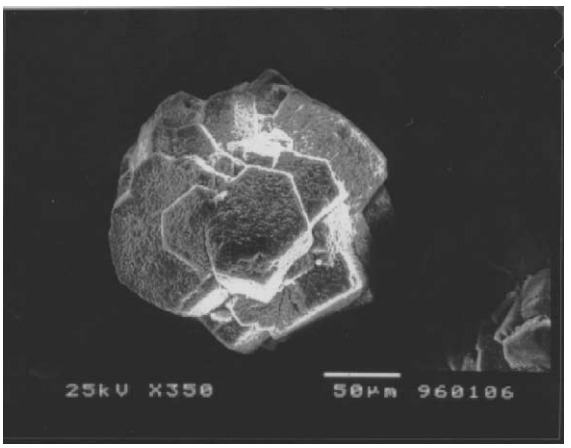

Fig. 6. The morphology of a typical agglomerate of the ceramics produced by the Sos synthesis.

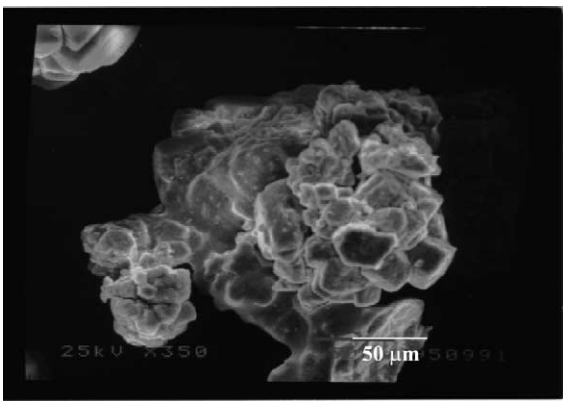

Fig. 7. The morphology of a typical agglomerate of the ceramics produced by the Per synthesis.

Table 2
Composition (wt% ± 1) of Sos and Per irradiated samples

Crystalline compound	Sos (wt%)	Per (wt%)
γ-$LiAlO_2$	0	90
α-$LiAlO_2$	100	7
Li_2O_2	0	<3
$LiH(AlO_2)_2 \cdot 5H_2O$	0	<3

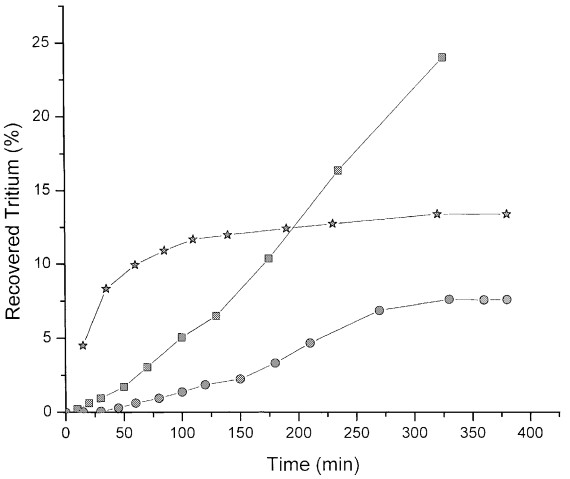

Fig. 8. Tritium recovery of Sos and Per samples. (■) Sos sample at 773 K; (★) Per sample at 773 K and (●) Per sample at 623 K.

Fig. 8 compares tritium released from Sos and Per samples at 773 K. As time increases, the Sos sample releases tritium at a lower rate than the Per sample which reaches a plateau after 70 min. After 300 min, the Sos sample tritium recovery was higher than the corresponding for the Per sample.

However, the recovery temperature determines the amount of recovered tritium, the sample at 623 K only reaches 8% after 380 min which is 59% of the plateau value in the same sample at 773 K.

4. Discussion

The synthesis methods used in this work reproduce the product distribution obtained by Frianeza-Kullberg et al. [22], Turner et al. [23], Schulz and Wedemeyer [24]. The solid-state reaction [22,24] (Sos) produces always

the purest γ-$LiAlO_2$ and the humid method [23] (Per) produces a mixture of γ- and α-$LiAlO_2$. Due to the amount of γ-$LiAlO_2$ provided by the solid-state preparation this synthesis route has been considered the most attractive for commercial processes. However, although humid methods produce complex mixtures, the resulting samples present high surface areas [23].

The value of the γ-$LiAlO_2$ *c* parameter obtained by Sos or Per methods differs from the *c* parameter value reported by Marezio. The value obtained in this work, 62.7 nm, indicates an expansion of the lattice in the *c*-direction. This difference is beyond the experimental error as all cell parameter values obtained for α-$LiAlO_2$ are identical to those of Marezio [8]. If a tetrahedron (AlO_2) is considered, where the center is occupied by an aluminum atom, the lithium atoms are located outside the tetrahedron and lithium enriched crystalline planes are found mainly in the *c*-direction. Lithium is, indeed, known to be weakly bonded to the spinel network, Jacobs et al. [25]. It seems, therefore, that our γ-$LiAlO_2$ (Sos or Per) is lithium enriched, independently of the purity of the mixture. Some of the lithium excess is constituted by interstitial atoms which in turn should propitiate the formation of superlattices. Under the Per synthesis conditions, the type of the formed superlattice is constituted by two phases with γ-$LiAlO_2$ as the principal phase and the α-$LiAlO_2$ as the secondary one.

Furthermore, the electron microscopy results show that synthesis methods may be correlated with the material microstructure. Although ceramics may present a long range crystalline order, their composition and structure may vary locally. The less ordered ceramic, in this sense, is the Sos sample even if it is purer. The presence of a well defined superlattice favors order in the Per ceramic. Then, the entropy of a Sos crystal is greater than in a Per crystal and, therefore, as expected, there are more lattice defects in the former sample.

The amount of lattice defects determines lithium or tritium diffusion. As tritium diffusion may be accelerated by point defects, it should vary depending on a Sos or Per environment. Several interactions may be expected; the strongest interaction occurs between impurity atoms and dislocations [26]. These impurities locally expand or contract the lattice depending on their size. Tritium is a substitutional impurity smaller than the matrix atoms that will segregate to the compressed region, and then, migrate to the core of an edge dislocation [27]; the dislocation is pinned by tritium. Sos should retain more tritium by this mechanism.

Superlattice presence favors the mobility of electrons and light elements through semiconductors as GaAs [28]. The same mechanism is expected in the diffusion and tritium release. Furthermore, the sample with the highest surface area presents the highest number of superlattices, most probably, a synergetic effect between both parameters enhances the tritium and lithium mobility. Moreover, it shows that in the lithium aluminate ceramic materials not only irradiation damage produces superlattices [12] but since the synthesis they are present in our Per compound.

The type of superlattices shown in this work should provide growth patterns of the crystal surface with specific features [29]. The morphology of Per and Sos samples has to be correlated with the growth patterns of the crystal surface (determined by the superlattice presence). The Sos morphology, only large hexagonal platelets whose surface is rough, reproduce the shape of the reported γ-$LiAlO_2$ obtained by the sol–gel technique [30]. In Per samples the particles have the same shape as Sos samples but the surface of the grains is now smooth. Hence, the γ-$LiAlO_2$ grains are covered by a second structure, α-$LiAlO_2$ as a second phase of the superlattice. Indeed, the α-$LiAlO_2$ due to its symmetry, has mechanical properties, as close packed slip planes, which propitiate a smooth surface as the faceting is much easier. Most probably in the case of Per structure we have obtained a layered ultrathin coherent structure [31,32].

The Per superlattices should promote the formation of a monocrystalline γ-phase. All α-$LiAlO_2$ formed superlattices with the γ-$LiAlO_2$, ensuring the structural stability of the compound. Such compounds are then expected to be more resistant to irradiation damages.

Therefore, in the Sos preparation, the lithium enriched γ-$LiAlO_2$ may be modified with irradiation, as the lithium excess will promote the superlattice formation. The interstitial atom excess promotes, indeed, the superlattice formation in AsGa [20] and intermetallic compounds [28,29]. Not only the recovery methods may determine the amount of the collected tritium [24], the synthesis and the pre-treatment (i.e., microstructural features) of the samples may also improve it. Most previous studies in this fine grained material would suggest that surface desorption reaction would be rate limiting, however, in Sos and Per samples not only this mechanism is operating, nanostructure (superlattice) propitiates another way of tritium release.

These features may be correlated with the experimental tritium recovery measured in our samples, on the one hand a clear effect of temperature was observed (Per sample at 773 K and 608 K) and on the other the preparation method determined not only the amount of recovered tritium but the shape of the curve. Temperature enhances the thermal vibration in the gas as well as in the ceramic lattice. Therefore, tritium driven by a temperature gradient crawls out easily. The tritium recovery in Per samples reaches a plateau which indicates that there is a limit for the tritium recovery. This result may be interpreted in terms of the structure and morphology of the Per samples. Tritium probably

comes from the α-$LiAlO_2$ crust present in the Per samples. As temperature is increased the number of layers contributing to the tritium recovery process increases.

If the tritium recovery in the 773 K samples (Sos and Per) is compared, the first striking difference is that in Sos sample tritium recovery is constant whereas in the Per sample after 150 min no more tritium is recovered. The bend over of the tritium release curve at 10% for the Per sample is very unusual [4,5]. To understand such behavior nanostructure samples can be consider. For irradiated Sos sample, all constituted by α-$LiAlO_2$ the operating mechanism is the tritium recovering from the bulk, not from the surface. As the irradiated Sos sample presents a large number of defects and vacancies, tritium moves hardly as it is trapped in these sites, until structure becomes ordered. The free tritium gets out the structure by the slip planes. For irradiated Per sample, the superlattice introduces more order in the α-$LiAlO_2$ crust. Tritium releases at first from this crust easier than from Sos sample, afterwards, tritium from the bulk is trapped and remains in the sample.

If a high amount of tritium has to be recovered a ceramic constituted by irradiated α-$LiAlO_2$ prepared by the Sos method is recommended, but if the time is short the Per synthesized sample can be more useful.

5. Conclusion

The γ-$LiAlO_2$ compound obtained either by the Sos and Per synthesis method was lithium enriched. Furthermore, it has been shown that preparation methods determine the presence of superlattices which can be compared to the superlattices observed under irradiation.

We have observed that the presence of the α-$LiAlO_2$ in the synthesis product introduces order in the Per sample through the ultrathin superlattice formation on the surface which determines the tritium recovery performance. Preparation method determines, then, the structure and morphology of the samples and therefore, curves of tritium recovery. Large amounts of tritium are obtained if the compound is α-$LiAlO_2$ and no linear defects or vacancies are present.

Acknowledgements

The technical help of J. Cañetas-Ortega (IFUNAM) in SEM observations is acknowledged. L.M.C. thanks the Conacyt for a postgraduate grant (858586516) and P.B. thanks the European Community (contract CI1*CT-94-0064) for financial help.

References

[1] L.W. Hobbs, F.W. Clinard, S.J. Zinkle, R.C. Ewing, J. Nucl. Mater. 215 (1994) 291.
[2] J.P. Kopasz, C.A. Seils, C.E. Johnson, J. Nucl. Mater. 212–215 (1994) 912.
[3] N.M. Masaki, K. Noda, H. Watanabe, R.G. Clemmer, G.W. Hollenberg, J. Nucl. Mater. 212–215 (1994) 908.
[4] H. Kwast, R. Conrad, R. May, S. Casadio, N. Roux, H. Werle, J. Nucl. Mater. 212–215 (1994) 1010.
[5] G. Federici, C.H. Wu, A.R. Raffray, R.C. Billone, J. Nucl. Mater. 187 (1992) 1.
[6] C.E. Johnson, K.R. Kummerer, E. Roth, J. Nucl. Mater. 155–157 (1988) 188.
[7] D. Yamaki, S. Tanaka, M. Yamawaki, J. Nucl. Mater. 212–215 (1994) 917.
[8] M. Marezio, Acta Crystallogr. 19 (1965) 396.
[9] M. Marezio, J.P. Remika, J. Chem. Phys. 44 (1966) 3143.
[10] J.L. Ethridge, PhD thesis, University of Washington, 1988.
[11] J. Charpin, F. Botter, M. Brieck, B. Rasneur, E. Roth, N. Roux and J. Sannier, Investigation of γ lithium aluminate as tritium breeding material for a fusion reactor blanket CEA-Conf-9482, 1988.
[12] M.H. Auvray-Gély, A. Dunlop, L.W. Hobbs, J. Nucl. Mater. 133&134 (1985) 230.
[13] L.M. Carrera, J. Jiménez-Becerril, P. Bosch, S. Bulbulian, J. Am. Ceram. Soc. 78 (1995) 933.
[14] R.S. Caswell, J.J. Coyne, M.L. Randolph, Rad. Res. 83 (1980) 217.
[15] ASTM E-261-90, Determining Neutron Fluency Rate, Fluency on Spectra by Radioactivation Techniques, USA, 1990.
[16] K. Tsuchiya, H. Kawamura, M. Saito, K. Tatenuma, M. Kainose, J. Nucl. Mater. 219 (1995) 246.
[17] Sakthivel, R.A. Young, User's guide to programs DBWS-9006 and DBWS-9006PC, Atlanta, GA, 1991.
[18] J. Schneider, User's guide manual to WYRIET3 computer program, Munich, Germany, 1993.
[19] Cerius^2, User's reference, release 2.0, BIOSYM/Molecular Simulations, USA, 1995.
[20] L. Esaki, in: G.W. Crabtree, P. Vashishta (Eds.), Novel Materials and Techniques in Condensed Matter, Plenum, New York, 1982, p. 1.
[21] D. Vollath, H. Wedemeyer, Adv. Ceram. 25 (1989) 93.
[22] T.C. Frianeza-Kullberg, D.P. McDonald, Ceram. Trans. (Ceram. Powder Sci. III) 12 (1990) 147.
[23] C.W. Turner, B.C. Clatworthy, A.Y.H. Gin, AECL-9614 (1987) 13.
[24] B. Schulz, H. Wedemeyer, J. Nucl. Mater. 139 (1986) 35.
[25] J.P. Jacobs, M.A. SanMiguel, L.J. Alvarez, P. Bosch, J. Nucl. Mater. 232 (1996) 131.
[26] R. Fuentes-Samaniego, W.D. Nix, G.M. Pound, Phil. Mag. A 42 (1980) 1339.
[27] W.D. Nix, R. Gasca-Neri, J.P. Hirth, Philos. Mag. 23 (1971) 1339.
[28] H. Gleiter, in: Materials Research Society Symposium Proceedings, 206, 1991, p. 463.
[29] T. Mukai, C. Kinoshita, S. Kitajima, Philos. Mag. A 47 (1983) 255.

[30] M.A. Valenzuela, J. Jiménez-Becerril, P. Bosch, S. Bulbulian, V.H. Lara, J. Am. Ceram. Soc. 79 (1996) 455.
[31] T.G. Gilbert, S.J. Gurman, Superlattices Microstructures 3 (1987) 17.
[32] M. Falco, I.K. Schuller, in: G.W. Crabtree, P. Vashishta (Eds.), Novel Materials and Techniques in Condensed Matter, Plenum, New York, 1982, p. 21.